Int J Earth Sci (Geol Rundsch) (2006) 95: 239–249
DOI 10.1007/s00531-005-0031-0

ORIGINAL PAPER

Kasper D. Fischer

The influence of different rheological parameters on the surface deformation and stress field of the Aegean–Anatolian region

Received: 25 March 2004 / Accepted: 13 June 2005 / Published online: 23 September 2005

Abstract The Aegean–Anatolian region is characterised by an inhomogeneous deformation pattern with high strain rates and a high seismicity both at the boundaries and in the plate interior. This pattern is controlled by the geometry and rheology of the structural units involved and their tectonic setting. A numerical analysis with a finite-element model of the region is used to quantify the influence of different rheological parameters. Viscoelastic material behaviour is implemented for the mantle lithosphere, whereas the crust is modelled with an elastic–plastic rheology. The variation of the inelastic material properties (viscosity and plastic strength) quantifies the influence of these material parameters on the deformation, stress, and strain patterns. Comparison of the modelled results with geodetic and geophysical observations reveals that the viscosity of the mantle lithosphere is the key to explaining the inhomogeneous deformation pattern. The best-fit model yields a viscosity of 10^{20} Pa s beneath Anatolia, whereas adjacent regions have viscosities between 10^{21} and 10^{23} Pa s. The model also explains the intra-plate seismicity and the stress field as well as its partitioning into regions with strike-slip and normal faulting. The final model is in good agreement with seismological, geodetic, and geological observations. Local deviations can be tracked down to small-scale structures, which are not included in the model.

Keywords Numerical model · Mantle viscosity · Eastern Mediterranean · Crustal deformation · Seismicity

K. D. Fischer (✉)
Institut für Geologie, Mineralogie und Geophysik,
Ruhr-Universität Bochum, NA 3/174,
44780 Bochum, Germany
E-mail: kasper.fischer@ruhr-uni-bochum.de
Tel.: +49-234-3227574
Fax: +49-234-3214181

Introduction

The Aegean Sea region, the adjacent part of the Greek mainland, and Turkey are strongly affected by the convergence among the African, Arabian, and Eurasian plates. This has lead to a strong deformation of the Aegean–Anatolian region since at least the Miocene time, which is mostly extensional as a result of the roll-back of the African plate along the Hellenic Subduction Zone and strongly affected by the extrusion of Anatolia (Gautier et al. 1999; Jolivet and Faccenna 2000). The Aegean–Anatolian region has been the subject of numerous studies, in particular geological studies (e.g. McKenzie 1972; ten Veen and Postma 1999; Jolivet and Faccenna 2000; Avigad et al. 2001; Koukouvelas and Aydin 2002; ten Veen and Kleinspehn 2003). The technological progress, especially in the field of satellite geodesy, yields valuable new observational constraints on the internal deformation of this region (e.g. Le Pichon et al. 1995; McClusky et al. 2000). Seismological studies revealed the internal crustal structure of the region and its seismicity (e.g. Papazachos et al. 1967, 2000a, b; Payo 1967, 1969; Papazachos 1969; Calcagnile et al. 1982; Kalogeras and Burton 1996; Papazachos and Nolet 1997; Alessandrine et al. 1997; Hearn 1999; Martinez et al. 2000; Li et al. 2003; Meier et al. 2004; Endrun et al. 2004). The results of these geological, geodetic, and seismological studies were the base for many numerical models (i.e. Armijo et al. 2004; Cianetti et al. 2001; Giunchi et al. 1996; Kreemer et al. 2004; Meijer and Wortel 1997; Provost et al. 2003). Most numerical studies dealt with the possible causes for the observed deformation and the influence of different boundary conditions on the deformation. Many of these models employ either rigid or deformable blocks connected along a-priori boundaries (e.g. known faults) and are constrained by only one observable (e.g. GPS derived velocities). A different approach and goal is followed in this study. The aim is to investigate the influence of the crustal strength and the viscosity of the

mantle lithosphere on many different independent observable parameters such as the deformation, stress field, and seismicity by a model, which accounts for internal inelastic deformation without a-priori defined faults or other internal boundaries. An exception is the North Anatolian Fault (NAF) that is a large-scale structural feature of the region, which developed over a long time span and is essential for the observed deformation field (McClusky et al. 2000). Nevertheless, the previous numerical models provide valuable constraints on the range of material parameters and boundary conditions.

Tectonic and geophysical constraints

For a numerical model of the Aegean–Anatolian region, it is necessary to understand the complex tectonic setting among the Eurasian, African, and Arabian plates (Fig. 1) and to include appropriate initial and boundary conditions in the model. The relative motion of these plates causes an overall convergent setting dominated by the westward counter-clockwise extrusion of Anatolia and the roll-back of the subducting African Slab. Both lead to a south-westward motion of the Aegean plate (Meijer and Wortel 1997).

The motion of Anatolia and western Turkey can be described by a rigid plate counter-clockwise rotation (McKenzie 1972; Bird 2003), which is bounded by the NAF in the north and the East Anatolian Fault (EAF) in the south-east. Large areas of this region show almost no internal deformation. Instead, the deformation is localised within small regions of large deformation, which are also visible in the distribution of epicentres (Fig. 2). The rigid motion of the Anatolian plate also affects the motion and internal deformation of the adjacent Aegean plate. This plate was first proposed by McKenzie (1972) and incorporated in a global plate tectonic model by Bird (2003). The Aegean plate generally moves south-westward overriding the African plate along the Hellenic Subduction Front. The first-order motion of both the plates, relative to a fixed Eurasian reference frame, can be described by a rotation around a common Euler pole. More detailed studies of GPS velocities reveal a small clockwise component of motion of the Aegean plate (LePichon et al. 1995; McClusky et al. 2000). Consequently, there must be a region of deformation between the Aegean and Anatolian rigid plates. These rigid plate models, however, do not account for internal deformation of the plates. The numerical model does not divide the region into different plates but uses an approach with one larger plate and takes internal deformation into account.

Observed deformation, seismicity, and stress field

The quality of the numerical models can be quantified when the calculated results are compared to observations. Many different data sets exist for the Aegean–Anatolian region that are of different spatial and temporal resolution and coverage. A data set has to fulfil the following criteria to be used as a reference for the modelling results. It should cover the modelled area, the spatial resolution of the data set has to be similar to the spatial resolution of the model, the observed data should be predictable by the numerical model, and the observed data should still be valid if extrapolated to longer time spans. The first criterion seems to be trivial, but is hard to fulfil particularly for regional studies.

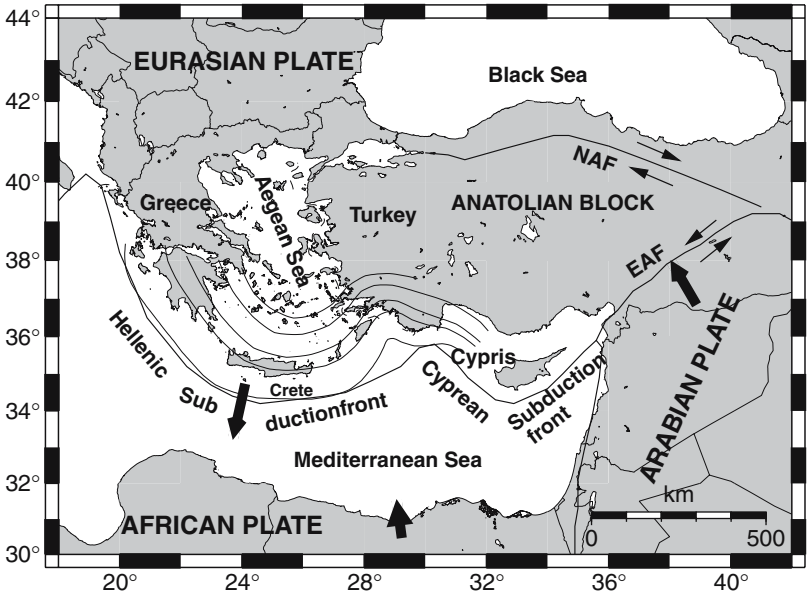

Fig. 1 The main tectonic features of the Eastern Mediterranean region. *Thick solid lines*: plate boundaries of the NUVEL-1A model (DeMets et al. 1994), North Anatolian Fault (NAF), and East Anatolian Fault (EAF), *thin lines*: slab depth contours (50 km interval, after Gudmundsson and Sambridge 1998), *arrows*: relative plate motions (not to scale, after McClusky et al. 2000)

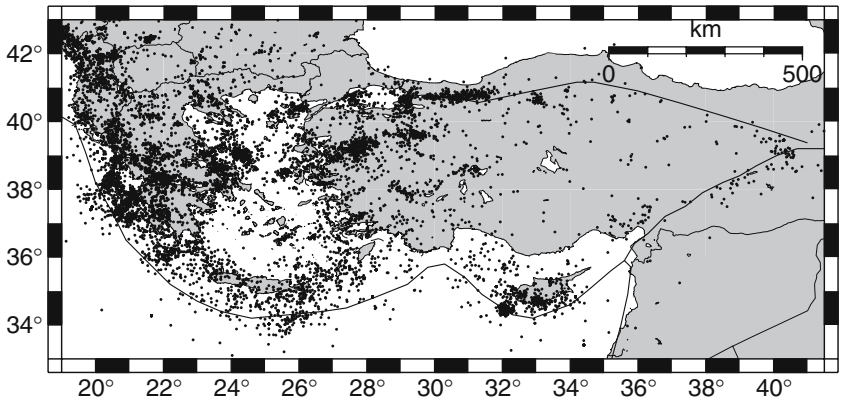

Fig. 2 The seismicity of the Aegean–Anatolian region from 1998 to 2003 in the upper 30 km of the crust (NEIC 2004). The events parallel to the Hellenic and Cyprean Arcs are related to the subduction of the African plate, which is not included in the numerical model. *Heavy solid lines*: plate boundaries of the NUVEL-1A model (DeMets et al. 1994) and the North Anatolian Fault (NAF)

GPS velocities

The first data set, which will be used as a reference for the calculated deformation, is the data set of GPS velocities published by McClusky et al. (2000). This data set covers the modelled area and extends over the model boundaries. The spatial resolution is similar to the modelled one and the velocity vectors can be easily calculated from the modelled displacement field. Thus, the quality of the model can be expressed by a misfit parameter $M = \sum |v_o - v_c| / (\sum |v_o| - \sum |v_c|)$, where v_o is the observed velocity and v_c is the calculated velocity. The observed velocity field (Fig. 3) is characterised by an overall counter-clockwise rotation of the Aegean–Anatolian plate (in a Eurasia-fixed reference frame) and an increase of magnitude from east to west. The velocities decrease to the north of the NAF and in the stable Greek mainland. McClusky et al. (2000) identified two Euler poles to describe the rotation of the Aegean and Anatolian plates, respectively. The two parts are divided by a region of large deformation and seismicity in western Turkey. The mainland of Greece is decoupled from this motion by the Korinth rift and an area of large deformation and seismicity in the northern Aegean Sea, which is interpreted as the westward extension of the NAF (i.e. Kokouvelas and Aydin 2002; Gautier et al. 1999; Le Pichon et al. 1995). McClusky et al. (2000) also compared the observed velocity field to geological constraints and drew the conclusion that the velocity field did not change significantly since the Pliocene (~4–5 Ma). Gautier et al. (1999) discuss the onset of extension for different metamorphic complexes of the Aegean and concluded that the Aegean extension started at least 20 Ma ago (lower Miocene) in a back-arc environment. To summarise, this indicates that the Aegean extension was already active on a large-scale before the onset of the collision of Arabia with Eurasia. This data set fulfils all the criteria defined above.

Seismicity

The large deformation of the area causes many earthquakes and the region is well known for its high seismicity (Makropoulos and Burton 1981; Papazachos et al. 2000a, b). Figure 2 shows the crustal seismicity of the years 1999–2003 as published in the NEIC database (NEIC 2004), which covers the whole modelled region. The seismic activity along the Hellenic and Cyprean subduction zones can readily be seen. The large number of events in the northern Aegean Sea and north-western Turkey is an expression of the large extensional and strike-slip deformation connected to the diffuse westward extension of the NAF. The observed seismicity cannot be compared directly to any calculated values since the numerical model does not include the brittle

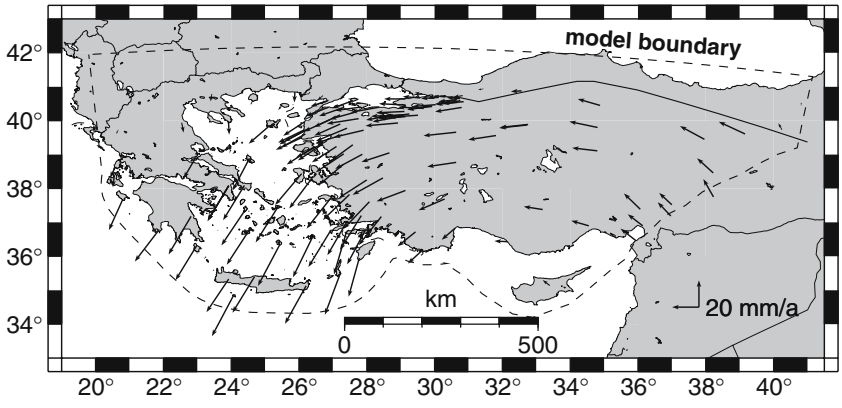

Fig. 3 The observed velocity field (Eurasian reference frame, data published by McClusky et al. 2000) of the Aegean–Anatolian plate within the model boundaries (*dashed line*). *Black line*: North Anatolian Fault (NAF)

behaviour of the material. The overall deformation by brittle failure is modelled by non-reversible plasticity instead. Thus, the calculated plastic strain can locate areas that might produce seismic events and this can be compared to the observed high intra-plate seismicity of the Aegean–Anatolian region. Whether the observed seismicity is representative for a large time-span or just a snapshot of the seismicity of the last few hundred or even only few tens of years is unknown. Even though this data set does not comply with all the criteria, it is still valuable to constrain the model and to interpret its results.

Stress field

The third data set to test against the numerical results is the stress field obtained from the 'World Stress Map Project' (WSM, Reinecker et al. 2003; Heidbach et al. 2004). The WSM database contains different stress values (direction of the largest horizontal stress and regime) from various data sets such as focal mechanisms, borehole breakouts, overcoring, hydrofractures, and geological indicators. This data can be compared with the calculated stress tensor from which the direction of the largest horizontal stress and the most likely faulting regime can be deduced (Reinecker et al. 2003; Yin and Ranalli 1992). The main feature is the partitioning of the region in parts dominated by strike-slip faults and by normal faulting. The spatial covering of the model area and the quality of the data set is not as good as it was for the other two data sets. It is also unknown whether the current stress field can be extrapolated over large time-spans. On the other hand, it can be compared directly with calculated stresses.

Numerical model

The Aegean–Anatolian region is modelled with the finite-element method using the commercial program Abaqus (Abaqus Inc., Providence, RI (USA)). It employs three-dimensional (3D) second order inelastic elements to calculate the deformation and stresses and their variation in time. Inelastic elements are capable of calculating the elastic and non-elastic material behaviour by separating the elastic components of the stress and strain from the non-elastic ones like creep and/or plastic yielding. The numerical model (Fig. 4) consists of five different blocks with an elastic–plastic crust and a viscoelastic mantle lithosphere. The descending African slab is not included in the model.

Geometry and boundary conditions

The five different blocks of the model cover the area of the Aegean Sea and Anatolia including the Greek mainland. It is bounded by the Hellenic Subduction Front and the Cyprean Subduction Front in the West and the South and the EAF in the East. The northern and north-western boundaries are defined arbitrarily by straight lines. They include the stable Eurasian plate. The outline of the model is included in Fig. 3. Figure 4 is a map view of the model including the five blocks and the applied boundary conditions. The total size of the model is about 1,780×500 km^2 with a thickness of 100 km. The Moho depth varies from 30 km below the Aegean Sea to 45 km below Anatolia (taken from the *Crust2.0* model, Bassin et al. 2000) and is at constant depth within each of the five blocks.

The model is constrained by different boundary conditions and forces acting on the model (Fig. 4). The obliquely subducting African lithosphere is not included in the model. Instead, the effect of the slab roll-back is taken into account by prescribing a velocity field along the Hellenic Subduction Front. Note that the applied velocities are not normal to the subduction front. This is clearly indicated by the observed GPS velocities (McClusky et al. 2000; Fig. 3). Determination of the local stress field based on focal mechanisms (M. Bohnhoff et al. submitted) also indicates a uniform relative plate motion at the Hellenic subduction front. All velocity boundary conditions of the model apply vertically from the top to the base of the model (i.e. the crust and mantle lithosphere). This model assumes that the deformation and stress field of the crust and mantle lithosphere are vertical coherent (Kreemer et al. 2004).

It is assumed that the Aegean–Anatolian region continuously deforms on the considered scale of this study except along the NAF. The NAF is included as a slip surface with an effective friction coefficient of 0.2. Investigations on coulomb stress changes between subsequent earthquakes along the NAF (Muller et al. 2003) and numerical models of the GPS velocity field along the NAF (Provost et al. 2003) indicate that an average effective friction coefficient of 0.2 is valid for the entire NAF.

Since time-dependent constitutional laws are employed, it is also necessary to include a proper timing of the evolution of the region into the model. Geological indicators show two relevant phases for modelling the overall deformation of the region (Gautier et al. 1999). The first phase was dominated by extensional deformation within the entire Aegean Sea caused by the roll-back of the African slab. The second phase commences with the onset of the collision of the Arabian plate with the Anatolian block, which influences the deformation of the Aegean Sea approximately since the last 4 Ma. The deformation propagated northward and focused on the northern Aegean Sea in this phase and the NAF developed its present shape (Jolivet and Faccenna 2000; Koukouvelas and Aydin 2002). Both phases are implemented in the model, but all calculated values are taken from the second phase only. Nevertheless, the first phase is included since the used rheologies are time-dependent and irreversible in time. It spans the time from 5 to 4 Ma before present to allow for the build up of a stress field

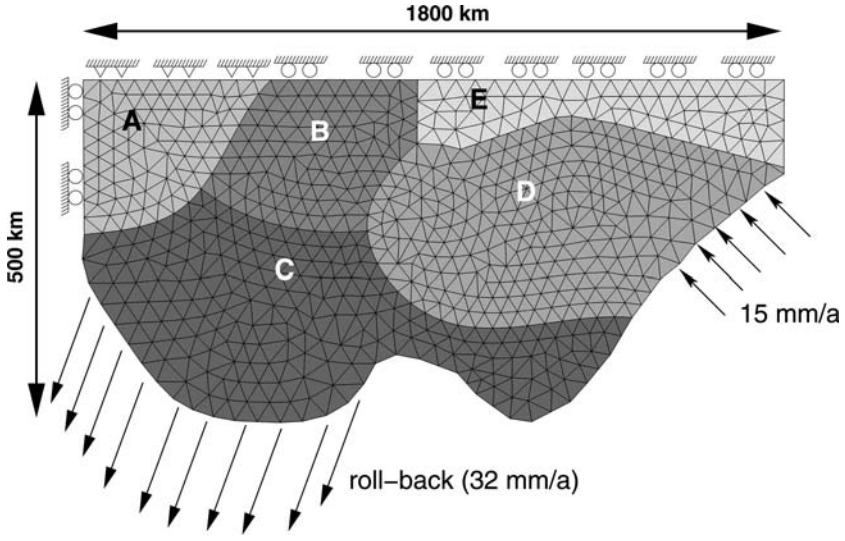

Fig. 4 The geometry of the numerical model and its boundary conditions (BC). The northern (*upper*) and western (*right*) edges have roller-style BC (movement only parallel to the edge allowed). The northern edge of block A is fixed. Displacement BC is applied along the Hellenic Arc and the East Anatolian Fault (32 and 15 mm/a, respectively). The model consists of five blocks divided into crust and mantle lithosphere with different thicknesses of the crust and mantle lithosphere: *A* 40 km Moho depth, *B* 30 km, *C* 30 km, *D* 45 km, and *E* 40 km (NAF). The edges of the model elements are approximately 45 km long. The total dimension of the model is approximately 1,780×500×100 km^3

close to the yield stress and continues for another 4 Ma in the second phase.

Rheology

The model layers have two different rheologies. The upper layer (crust) is modelled with a plastic–elastic rheology and the lower layer (mantle lithosphere) with a viscoelastic constitutive law. Both layers are calculated with temperature independent rheologies, but the chosen material properties take into account different temperatures of the crust and mantle at different depths and locations. This is done by using different static temperature independent values for the material at different depths or temperatures. This model assumes that the temperature of the lithosphere does not change significantly during the modelled time-span.

The plastic–elastic rheology of the crust follows a linear Drucker–Prager material law with strain hardening. Its behaviour can be described by pure elastic deformation up to the yield stress σ_y. The yield stress σ_y is a function of internal material parameters (the friction angle β), the strain hardening d, and the local pressure p: $\sigma_y = d + p \tan\beta$. The strain hardening parameter d depends on the total plastic strain and is modelled with a value of 70 MPa for zero plastic strain and 70 GPa for plastic strains of 0.7.

The Drucker–Prager model is similar to the well-known Mohr–Coulomb law (Drucker and Prager 1952) and has some numerical advantages. The important difference is that the friction angles β of the Drucker–Prager model are in general larger than the angle of Coulomb friction ϕ of the Mohr–Coulomb model. The numerically important difference is that the three-dimensional yield surface in the principal stress space of the Drucker–Prager model is smoother than that of the Mohr–Coulomb model (Zienkiewicz and Taylor 2000).

The viscoelastic behaviour of the mantle lithosphere involves a stress-dependent creep in addition to the normal pure elastic response. The creep strain-rate $\dot{\varepsilon}$ can be calculated from the material viscosity η and the shear stress σ by the relation $\dot{\varepsilon} = (1/2\eta)\sigma$. This is a simple case of linear creep.

The material properties are taken from seismological studies and are compiled in the seismic model *Crust2.0* (Bassin et al. 2000). It provides values for the Moho depth, the average crustal density, the density of the mantle lithosphere, and P- and S-velocities of the crust and mantle lithosphere, respectively. The elastic material parameters E (Young's modulus) and ν (Poisson's ratio) can be calculated directly from these seismic values (Table 1). The inelastic material properties of the crust (friction angles β and strain hardening d) and the mantle lithosphere (viscosity η) are more uncertain. The viscosity η is varied from 10^{18} to 10^{26} Pa s and the friction angle β from 37° to 50.5°. The range of the values is constrained by results published by Ranalli (2000), Hearn et al. (2002), and Gerya et al. (2002). The different values are summarised in Table 1. Different combinations of these parameters were used to calculate the deformation with the goal to obtain a good fit between the calculated deformation and stress field and the observed values. The aim of the model is to pinpoint the values of the material properties for the Aegean–Anatolian region for further studies and to provide a better understanding of the deformation, stress, and strain field as well as of results from seismological studies

(e.g. Papazachos and Nolet 1997; Meier et al. 2004). Table 1 gives an overview of the different rheological parameters.

Results

Deformation

The first analysis of the model results addresses the deformation of the blocks and their dependence on the mantle viscosity in the blocks. Calculations were done for over 50 different combinations of viscosity values ranging from 10^{18} to 10^{26} Pa s (Table 1). The changes in horizontal displacement from the beginning to the end of the second phase were used to calculate average velocities. These velocities are compared to the observed velocities from GPS observations by McClusky et al. (2000) and used to calculate the misfit M. Figure 5 shows the typical velocity field of one of the calculated models and the one published by McClusky et al. (2000). One can clearly see that the overall deformation of the model matches the GPS observations. A more detailed view can be obtained when looking at the residuals (Fig. 5b), which reveals that the largest differences occur in the centre of the model at the edge between the model blocks C and D. Figure 6a–i shows the residual velocities for nine out of more than 50 analysed combinations and their dependence on mantle viscosity. The values were systematically varied in the first step to find the minimal misfit. In a second step, the calculated combinations were limited in range to pinpoint the minimal misfit in the neighbourhood of the best parameter combinations of the first step.

Since the largest deviations occur in the region of the Marmara Sea, a misfit value $\tilde{M}$ excluding the observations in this area was calculated. The mean difference of $\tilde{M}$ and M is 0.034. The model with the smallest misfit value ($M = 0.196$) has a low viscosity (10^{18} Pa s) below Anatolia and a high viscosity (10^{24} Pa s) below the Aegean Sea, but models with a smaller contrast in viscosity show only a slightly larger misfit. One of these models has a misfit value of $M = 0.198$ ($\tilde{M} = 0.165$) and a viscosity of 10^{20} Pa s below Anatolia and 10^{21} Pa s below the northern Aegean, whereas all the other viscosities are 10^{22} Pa s (Fig. 6e). Uniform models having the same viscosity in each block have a misfit value of $M = 0.388$ (10^{20} Pa s), $M = 0.259$ (10^{21} Pa s), and $M = 0.245$ (10^{22} Pa s).

The best-fit model with viscosities of 10^{22} Pa s in blocks A, C, and E, 10^{20} Pa s in block D, and 10^{21} Pa s in block B was chosen to investigate the influence of different plasticity values of the crust on the deformation and stress field in a second step. Different models with friction angles β ranging from 37° to 50.5° were analysed. Even though no significant change of the surface displacement field could be found, they differ in the amount of inelastic energy released.

Stress field and seismicity

In addition to examining the deformation, the influence of different rheological properties on the stress field is investigated. Figure 7 shows the calculated stress field of the model and the stresses from the WSM project (Reinecker et al. 2003; Heidbach et al. 2004) for comparison. The symbols in these figures indicate the direction of the largest horizontal stress. The stress is defined in a way that positive stresses are extensional.

All models predict almost the same stress field with only minor variations in the direction of the largest horizontal stress and fit the observed stress field deduced from focal mechanisms. Figure 7b shows that the model is divided into two regions with different stress regimes. The southern Aegean Sea is dominated by normal faulting, whereas the remaining model is dominated by strike-slip faults. One should keep in mind that the shown regime of the modelled stress values gives the most likely faulting mode in an unfractured isotropic media and not whether faulting will occur at all or what mechanism will actually be generated. Especially in the region of the Menderes Massif (western Turkey), where many faults are observed, the assumption of an unfractured isotropic medium is not valid and leads to significant deviations from the predicted focal mechanisms.

Table 1 Rheological properties of the crust and mantle lithosphere for the five blocks of the numerical models. The shown values give the range used for the different calculated models. The elastic values (Young's modulus, Poisson's ratio, and density) are adopted from the seismological model *Crust2.0* (Bassin et al. 2000). The range of the inelastic values is used to find the best-fit model

Block	Young's modulus (GPa)	Poisson's ratio	Density (kg m^{-3})	Internal friction angle	Viscosity (Pa s)
Crust					
A	59.5	0.270	2,810	44.0°	
B	54.0	0.276	2,790	37.0–50.5°	
C	48.0	0.280	2,810	37.0–50.5°	
D	61.0	0.260	2,830	37.0–50.5°	
E	63.0	0.260	2,860	44.0°	
Mantle lithosphere					
A	117.0	0.250	3,300		10^{21}–10^{23}
B	117.0	0.250	3,300		10^{18}–10^{24}
C	126.5	0.255	3,400		10^{18}–10^{26}
D	119.0	0.250	3,350		10^{18}–10^{24}
E	114.0	0.260	3,300		10^{20}–10^{24}

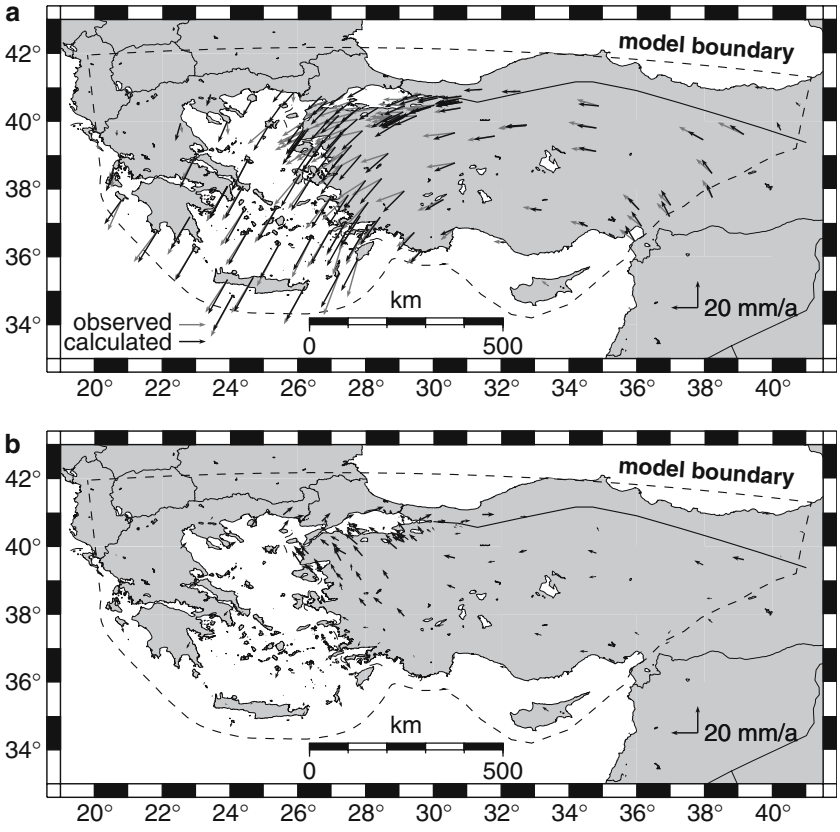

Fig. 5 The calculated velocity field of the final model compared to the observed velocities (McClusky et al. 2000). **a** Absolute calculated (*black*) and observed (*grey*) velocity vectors in a Eurasian reference frame. **b** Residual velocity field. *Dashed line*: model boundary, *black line*: North Anatolian Fault (NAF)

The area of the model where brittle faulting is possible is limited to regions with plastic deformation (Fig. 8). Regions with large plastic strains can be identified as regions with a high seismic activity (Fig. 2). The seismicity along the plate boundaries and the NAF does not correlate with high plastic straining since the subducting slab is not included and the frictional energy release at the NAF does not produce plastic deformation along the fault in the model.

Discussion and conclusions

The results demonstrate that the overall observed deformation and stress pattern can be reconstructed by the model and reveal their dependence on the different rheological properties. The parameter studies can clearly identify the strong dependence of the total deformation on the viscosity of the mantle lithosphere beneath Anatolia. It must be as low as 10^{20} Pa s, and thus it is significantly smaller (by a factor of 10–1,000) than that of the surrounding mantle lithosphere. This is supported by a seismic dispersion analyses (Meier et al. 2004) that indicate low P- and S-wave velocities below central Turkey. A more qualitative discussion of the strength of the mantle lithosphere by McClusky et al. (2000) also argues for this result. The low viscosity of the mantle lithosphere leads to a decoupling of the forces acting on the mantle lithosphere and the forces acting on the crust and might be the key to understand the tectonics of western Turkey and the Anatolian block.

Variations of the viscosity of the other blocks have a lower impact on the misfit parameter M and the deformation and stress fields. Some models indicate that the southern Aegean has a slightly larger viscosity (by a factor of 10–100) than the surrounding regions. It has to be investigated whether this is the true viscosity of the mantle lithosphere in this region or a result of the simplified geometry of the model, which does not include the descending African slab or related vertical forces (e.g. buoyancy).

Rheology also plays a very important role for the deformation of the northern Aegean Sea and the development of the high seismicity in this region. The steady straining of this region and its rather low yield strength leads to large inelastic (plastic) deformation. This is expressed as a large plastic strain component of the total strain in the model and a high intra-plate seismicity of the region in conjunction with the development of complex fault systems in the area of the northern Aegean Sea and western Turkey. The quantification of the influence of the crustal strength is not possible since it is not clear how much of the plastic deformation energy is released seismically or aseismically.

The third measure of quality is the fit of the calculated stress field that proved to be in good agreement with the observed stress field regarding the direction of

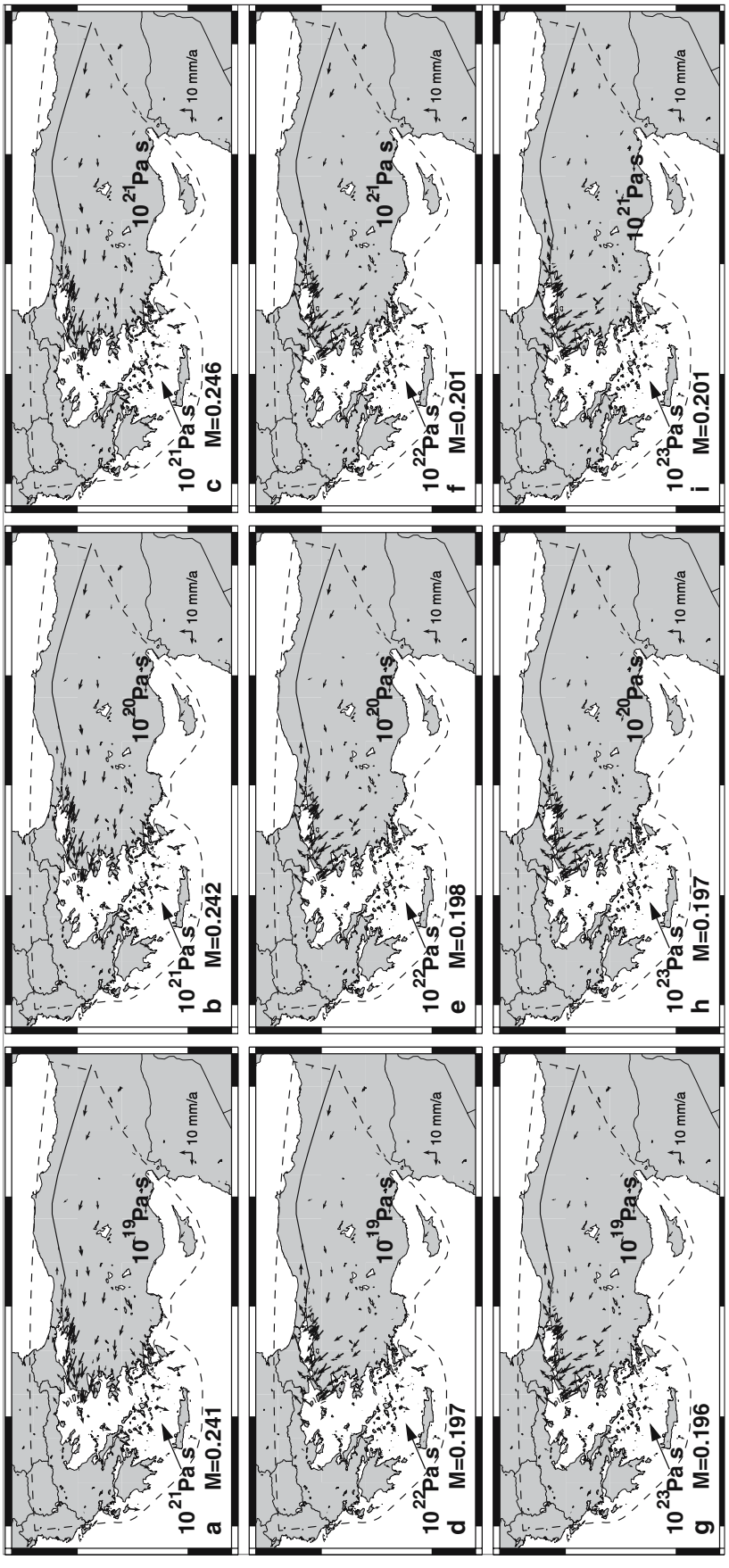

Fig. 6 Example of calculated velocity residuals for nine different viscosity combinations of the mantle lithosphere in blocks *C* and *D* (Fig. 4). Part **h** is the same as Fig. 5b. The calculated misfit parameter and the viscosity of blocks *C* and *D* are indicated in the figure. The remaining three blocks have a viscosity of 10^{22} Pa s (*A*,*E*) and 10^{21} Pa s (*B*). The mapped area is the same as in Fig. 5

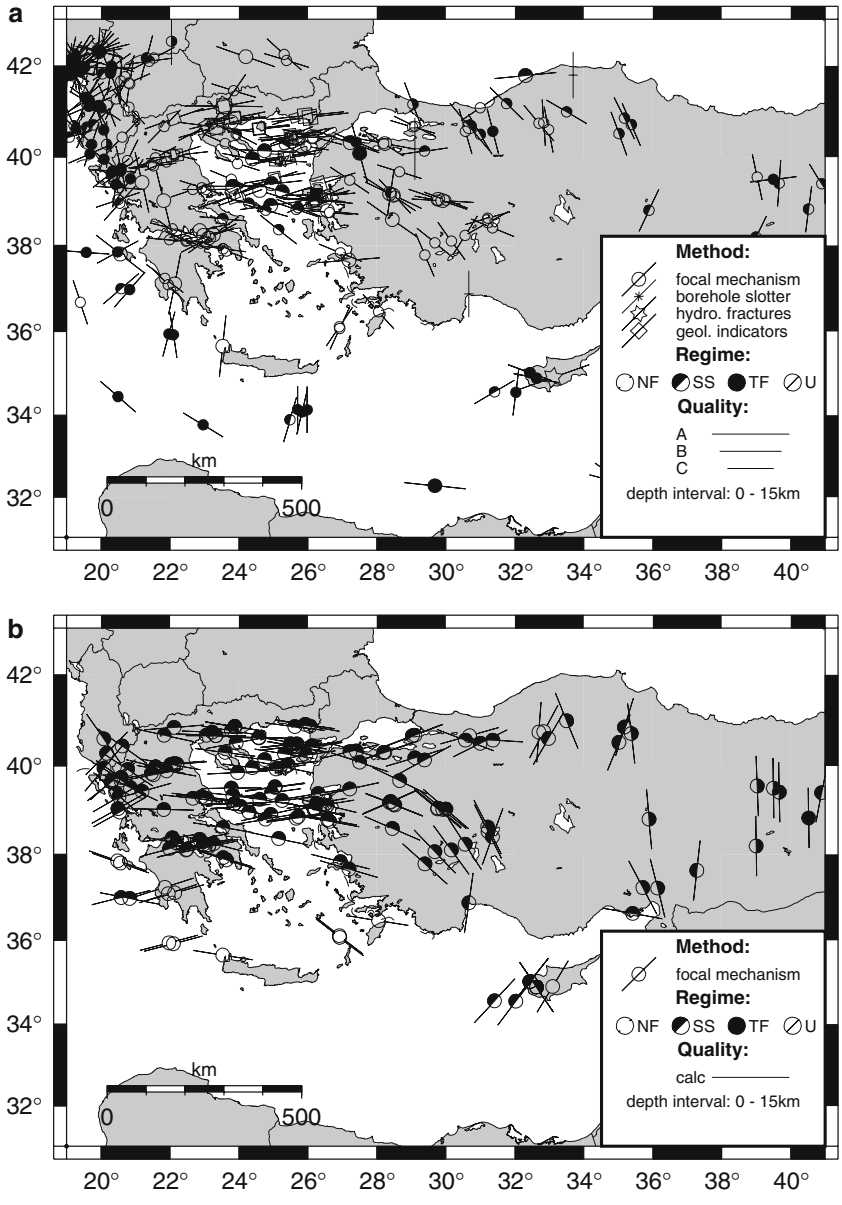

Fig. 7 a The stress field of the Aegean–Anatolian region from the World Stress Map project (WSM, Reinecker et al. 2003; Heidbach et al. 2004). **b** The calculated stress field at the same locations of the model shown in Fig. 6e. The directions of the symbols indicate the direction of the largest horizontal stress axis (positive stresses are extensional). The quality of the WSM database ranks from A (good) to D (poor, not plotted)

the principal stress axes. The direction of the principal stress axis is independent of the rheology of the crust and the mantle lithosphere in contrast to the deformation pattern and the amount of plastic straining. The direction mainly depends on the boundary conditions, that is, the tectonic setting.

There are also same large discrepancies between the modelled results and the observed data, which have to be discussed and investigated in further studies. These discrepancies are (1) the large deviations of the calculated velocities compared to the GPS observations at the western end of the NAF and (2) the wrong predicted faulting regime in western Turkey (Menderes Massif). Both discrepancies can be explained by the simplification of the complex fault structures and the neglect of local geological structures in the model. Especially, pre-existing faults will change the predicted stress regime and will lead to local deviations from the overall displacement field.

Besides a parameter study on constraining the mantle lithosphere's viscosity, a second parameter study was carried out to investigate the role of the crust's strength. One reason was to check whether a similar fit of the calculated to the observed deformation field could be obtained by just varying the crustal strength. There are some numerical studies that indicate that this might be possible like the one by Cianetti et al. (2001). However, they neither included the mantle lithosphere in their model nor compared their results with the observed stress field or seismicity. The numerical model presented here shows that a lateral variation of crustal strength is not sufficient to explain the observed GPS velocity field, the principal stress directions, and the intra-plate seismicity of the region. From the numerical results shown

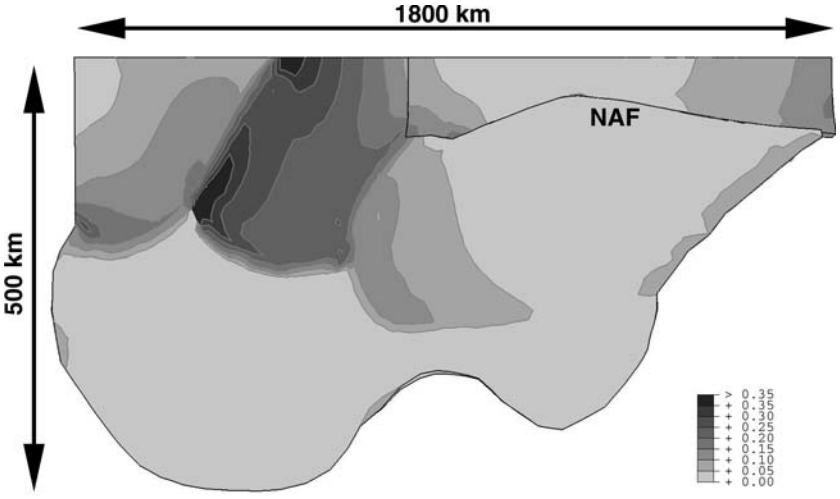

Fig. 8 Magnitude of the plastic strain (dimensionless) of the model shown in Fig. 6e. The plastic strain spans a range from 0.00 to above 0.35 of relative straining. Plastic deformation is concentrated at blocks *A*,*B*, and the western part of block *D*. These parts are characterised by high intra-plate seismicity (Fig. 2). Events at the plate boundary do not show up as plastic strain since the inter-plate coupling of the Eurasian and African plates is not included in the model. The seismicity along the NAF is not associated with plastic strain since the NAF is modelled with contact surfaces and, therefore, can only produce frictional energy release but no plastic deformation

here and from those of Kreemer et al. (2004), it follows that the thick mantle lithosphere controls the deformation, whereas the rheological properties of the crust influence the seismic energy release and has only limited influence on the principal stress directions.

Acknowledgements The author wants to thank the members of the 'Seismology Working Group' of H.-P. Harjes and of the collaborative research centre (SFB 526) 'Rheology of the Earth—from the upper crust to the subduction zone' of the Ruhr-University of Bochum for the many hours of discussion and valuable comments on this paper. This research would have not been possible without these people. Helpful comments of M. Bohnhoff (GFZ Potsdam), Th. Meier (U Bochum), J. Martinod, and an anonymous reviewer on the first version of this article are gratefully acknowledged.

References

Alessandrini B, Beranzoli L, Drakatos G, Falcone C, Kaantonis G, Mele MM, Stavrakakis GN (1997) Tomographic image of the crust and the uppermost mantle of the Ionian and the Aegean regions. Ann Geofis XL:151–160

Armijo R, Flerit F, King G, Meyer B (2004) Linear elastic fracture mechanics explains the past and present evolution of the Aegean. Earth Planet Sci Lett 217:85–95. DOI 10.1016/S0012-821X(03)00590-9

Avigad D, Ziv A, Garfunkel Z (2001) Ductile and brittle shortening, extension-parallel folds and maintenance of crustal thickness in the central Aegean (Cyclades, Greece). Tectonics 20:277–287. DOI 10.1029/2000TC001190

Bassin C, Laske G, Masters G (2000) The current limits of resolution for surface wave tomography in North America. EOS Trans AGU 81:897

Bird P (2003) An updated digital model of plate boundaries. Geochem Geophys Geosyst (G^3) 4:1027. DOI 10.1029/2001GC000252

Calcagnile G, D'Ingeo F, Farrugia P, Panza GF (1982) The lithosphere in the central-eastern Mediterranean area. Pure Appl Geophys 120:389–406

Cianetti S, Gasperini P, Giunchi C, Boschi E (2001) Numerical modelling of the Aegean–Anatolian region: geodynamical constraints from observed rheological heterogeneities. Geophys J Int 146:760–760. DOI 10.1046/j.1365-246X.2001.00492.x

DeMets C, Gordon RG, Argus DF, Stein S (1994) Effect of recent revisions to the geomagnetic reversal time scale on estimates of current plate motions. Geophys Res Lett 21:2191–2194. DOI 10.1029/94GL02118

Drucker DC, Prager W (1952) Soil mechanics and plastic analysis or limit design. Q J Appl Math 10:157–165

Endrun B, Meier T, Bischoff M, Harjes HP (2004) Lithospheric structure in the area of Crete constrained by receiver functions and dispersion analysis of Rayleigh phase velocities. Geophys J Int 158:592–608 DOI 10.1111/j.1365-246X.2004.02332.x

Gautier P, Brun JP, Moriceau R, Sokoutis D, Martinod J, Jolivet L (1999) Timing, kinematics and cause of Aegean extension: a scenario based on a comparison with simple analogue experiments. Tectonophysics 315:31–72. DOI 10.1016/S0040-1951(99)00281-4

Gerya TV, Stöckhert B, Perchuk AL (2002) Exhumation of high-pressure metamorphic rocks in a subduction channel: a numerical simulation. Tectonics 21(6):1056. DOI 10.1029/2002TC001406

Giunchi C, Kiratzi A, Sabadini R, Louvari E (1996) A numerical model of the Hellenic subduction zone: active stress field and sea-level changes. Geophys Res Lett 23:2485–2488. DOI 10.1029/96GL02166

Gudmundsson Ó, Sambridge M (1998) A regionalized upper mantle (RUM) seismic model. J Geophys Res 103:7121–7136. DOI 10.1029/97JB02488

Hearn TM (1999) Uppermost mantle velocities and anisotropy beneath Europe. J Geophys Res 104:15123–15139. DOI 10.1029/1998JB900088

Hearn EH, Hager BD, Reilinger RE (2002) Viscoelastic deformation from North Anatolia fault zone earthquakes and the eastern Mediterranean GPS velocity field. Geophys Res Lett 29(11):44. DOI 10.1029/2002GL014889

Heidbach O, Barth A, Connolly P, Fuchs K, Müller B, Tingay M, Reinecker J, Sperner B, Wenzel F (2004) Stress maps in a minute: the 2004 World Stress Map release. EOS Trans 85(49):521, 529

Jolivet L, Faccenna C (2000) Mediterranean extension and the Africa-Eurasia collision. Tectonics 19:1095–1106. DOI 10.1029/2000TC900018

Kalogeras IS, Burton PW (1996) Shear-wave velocity models from Rayleigh-wave dispersion in the broader Aegean area. Geophys J Int 125:679–695

Koukouvelas IK, Aydin A (2002) Fault structure and related basins of the North Aegean Sea and its surroundings. Tectonics 21:1046. DOI 10.1029/2001TC901037

Kreemer C, Chamot-Rooke N, Le Pichon X (2004) Constraints on the evolution and vertical coherency of deformation in the Northern Aegean from a comparison of geodetic, geologic and seismological data. Earth Planet Sci Lett 225:329–346. DOI 10.1016/j.epsl.2004.06.018

Le Pichon X, Chamot-Rooke N, Lallemant S, Noomen R, Veis G (1995) Geodetic determination of the kinematics of central Greece with respect to Europe—implications for eastern Mediterranean tectonics. J Geophys Res 100:12675–12690. DOI 10.1029/95JB00317

Li X, Bock G, Vafidis A, Kind R, Harjes HP, Hanka W, Wylegalla K, van der Meijde M, Yuan X (2003) Receiver function study of the Hellenic subduction zone: imaging crustal thickness variations and the oceanic Moho of the descending African lithosphere. Geophys J Int 155:733–748. DOI 10.1046/j.1365-246X.2003.02100.x

Makropoulos KC, Burton PW (1981) A catalogue of seismicity in Greece and adjacent areas. Geophys J R Astron Soc 65:741–762

Martinez MD, Lana X, Canas JA, Badal J, Pujades L (2000) Shear-wave velocity tomography of the lithosphere–asthenosphere system beneath the Mediterranean area. Phys Earth Planet Inter 122:33–54. DOI 10.1016/S0031-9201(00)00185-0

McClusky S, Balassanian S, Barka A, Demir C, Ergintav S, Georgiev I, Gurkan O, Hamburger M, Hurst K, Kahle H, Kastens K, Kekelidze G, King R, Kotzev V, Lenk O, Mahmoud S, Mishin A, Nadariya M, Ouzounis A, Paradissis D, Peter Y, Prilepin M, Reilinger R, Sanli I, Seeger H, Tealeb A, Toksoz MN, Veis G (2000) Global positioning system constraints on plate kinematics and dynamics in the eastern Mediterranean and Caucasus. J Geophys Res 105:5695–5719. DOI 10.1029/1999JB900351

McKenzie DP (1972) Active tectonics of the Mediterranean region. Geophys J R Astron Soc 30:109–185

Meier T, Dietrich K, Stöckhert B, Harjes HP (2004) One-dimensional models of shear-wave velocity for the eastern Mediterranean obtained from the inversion of Rayleigh wave phase velocities and tectonic implications. Geophys J Int 156:45–58. DOI 10.1111/j.1365-246X.2004.02121.x

Meijer PT, Wortel MJR (1997) Present-day dynamics of the Aegean region: a model analysis of the horizontal pattern of stress and deformation. Tectonics 16:879–895

Muller JR, Aydin A, Maerten F (2003) Investigating the transition between the 1967 Murdurnu Valley and 1999 Izmit earthquakes along the Northern Anatolian fault with static stress changes. Geophys J Int 154:471–482. DOI 10.1046/j.1365-246X.2003.01968.x

National Earthquake Information Center (NEIC) (2004) Preliminary determinations of epicenters. United States Geological Service. Available online at http://neic.usgs.gov/neis/epic/epic.html

Papazachos BC (1969) Phase velocities of Rayleigh waves in southeastern Europe and eastern Mediterranean Sea. Pure Appl Geophys 75:47–55

Papazachos BC, Nolet G (1997) P and S deep velocity structure of the Hellenic area obtained by robust nonlinear inversion of travel times. J Geophys Res 102:8349–8367. DOI 10.1029/96JB03730

Papazachos BC, Polatou M, Mandalos N (1967) Dispersion of surface waves recorded in Athens. Pure Appl Geophys 67:95–106

Papazachos BC, Comninakis PE, Karakaisis GF, Karakostas BG, Papaioannou CA, Papazachos CB, Scordilis EM (2000a) A catalogue of earthquakes in Greece and surrounding area for the period 550 B.C.–1999. Publ. of Geophys. Laboratory, Univ. of Thessaloniki, Greece

Papazachos BC, Karakostas VG, Papazachos CB, Scordilis EM (2000b) The geometry of the Wadati-Benioff zone and lithospheric kinematics in the Hellenic arc. Tectonophysics 319:275–300. DOI 10.1016/S0040-1951(99)00299-1

Payo G (1967) Crustal structure of the Mediterranean Sea by surface waves. Part I: Group velocity. Bull Seism Soc Am 57:151–172

Payo G (1969) Crustal structure of the Mediterranean Sea by surface waves. Part II: Phase velocity and travel times. Bull Seism Soc Am 59:23–42

Provost AS, Chéry J, Hassani R (2003) 3D mechanical modeling of the GPS velocity field along the North Anatolian fault. Earth Planet Sci Lett 209:361–377. DOI 10.1016/S0012-821X(03)00099-2

Ranalli G (2000) Rheology of the crust and its role in tectonic reactivation. J Geodyn 30:3–15

Reinecker J, Heidbach O, Mueller B (2003) The 2003 release of the World Stress Map. Available online at http://www.world-stress-map.org

ten Veen JH, Kleinspehn KL (2003) Incipient continental collision and plate-boundary curvature: late Pliocene-Holocene transtensional Hellenic forearc, Crete, Greece. J Geol Soc (Lond) 160:161–181

ten Veen JH, Postma G (1999) Roll-back controlled vertical movements of the outer-arc basins of the Hellenic subduction zone (Crete, Greece). Basin Res 11:243–266

Yin ZM, Ranalli G (1992) Critical stress differences, fault orientation and slip direction in an isotopic rocks under non-Andersonian stress systems. J Struct Geol 14(2):237–244

Zienkiewicz OC, Taylor RL (2000) The finite element method. Butterworth-Heinemann, Oxford, Great Britain